Macromolecules

ARTICLE

pubs.acs.org/Macromolecules

A Simple Reverse Mapping Procedure for Coarse-Grained Polymer Models with Rigid Side Groups

Azadeh Ghanbari,* Michael C. Böhm, and Florian Müller-Plathe

Eduard-Zintl-Institut für Anorganische und Physikalische Chemie and Center of Smart Interfaces, Technische Universität Darmstadt, Petersenstrasse 20, D-64287 Darmstadt, Germany

ABSTRACT: This article introduces a simple and fast method to reinsert atomistic details into mesoscale models of polymers with rigid side groups. We describe our backmapping scheme from a coarse-grained (CG) resolution to an atomistic picture in the framework of molecular dynamics (MD) simulations of a silica−atactic polystyrene (PS) composite. The CG model of Qian et al. [Macromolecules 2008, 41, 9919] has been used in the coarse-graining; it combines the atoms of one repeat unit of PS to a CG bead. In the reverse mapping only the centers of mass of these units and their chiralities are known. We show that this information is sufficient for the reverse mapping which requires simple geometrical and mechanical considerations. The capability of the suggested method is demonstrated by comparing MD results from the original atomistic model with those emerging from the reverse mapping. Because of its simplicity, the suggested technique offers the opportunity to study relaxed structures of melt chains with large molecular weights.

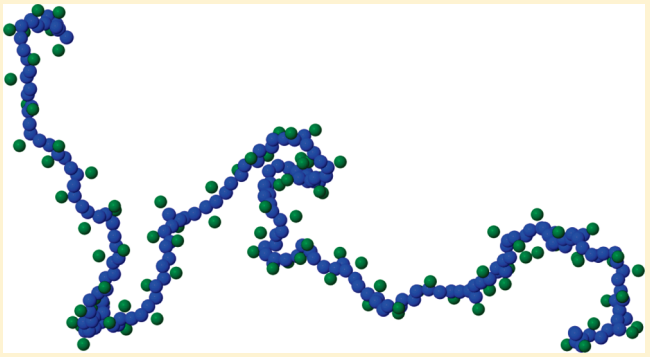

INTRODUCTION

The investigation of structure−property relations of polymeric materials by computer simulations requires the preparation of well-equilibrated melts. Large length and time scales of polymer melts can be reached by molecular dynamics (MD) and Monte Carlo (MC) variants in a so-called coarse-grained (CG) resolution, where groups of atoms are lumped together into superatoms or beads. Coarse-graining reduces the degrees of freedom to those which are assumed to be relevant for the quantities of interest.[1,2] During recent years different CG mapping schemes for polystyrene (PS) have been developed.[3−7] The CG procedures described for PS differ in the number of atoms considered in the definition of the beads as well as in the chosen bead center (the center-of-mass of the monomers or a certain atom are possible choices).[3−9] Although many quantities of complex polymer materials can be analyzed already in the CG picture, there are others where an atomistic resolution is necessary. The correlation between measured neutron diffraction data and calculated MD or MC ones is one important example.[10,11] Structural implications of absolute configurations of atoms or the determination of the orientation of ring fragments are other examples requiring atomistic simulation results. Thus, there is a need to transform CG representations of a given system back into an atomistic resolution once the relaxation and equilibration of the CG sample have been performed. This process of introducing atomistic details into a CG simulation is denoted as backmapping (BM) or reverse mapping. The variety of CG mappings implies of course the same variety in the reverse mapping schemes. Depending on the degree of coarse-graining, information on more or fewer atomic positions is lost. Hence, the demands on BM are predetermined by the type of coarse-graining. It is the purpose of the present contribution to introduce—in the framework of molecular dynamics simulations—a backmapping scheme for coarse-grained atactic polystyrene that is in contact with silica surface. This research has been motivated by our present computer simulations of silica−PS nanocomposites, where the mapping scheme of Qian et al.[3] has been used for the PS. A convenient BM procedure for the adopted CG scheme is the prerequisite to correlate CG simulations results with both atomistic data and various experimental results. Detailed studies of these samples are left for a forthcoming publication.

SYSTEM AND COMPUTATIONAL CONDITIONS

In the present article we have employed the scheme of Qian et al.[3] for coarse-graining atactic PS, the polymer component of a silica−PS nanocomposite. In this mapping scheme each repeat unit of PS is represented by one CG bead, located at the repeat unit's center-of-mass, and is called a (1:1) mapping. This CG model has two different beads (R and S) for repeat units of different chirality in order to describe tacticity. Milano et al.[4] proposed another (1:1) mapping scheme for PS which still conserves the underlying atomistic backbone, as the centers of the beads coincide with backbone-atom position. Santangelo et al.[10]

Received: March 15, 2011
Revised: May 27, 2011
Published: June 15, 2011

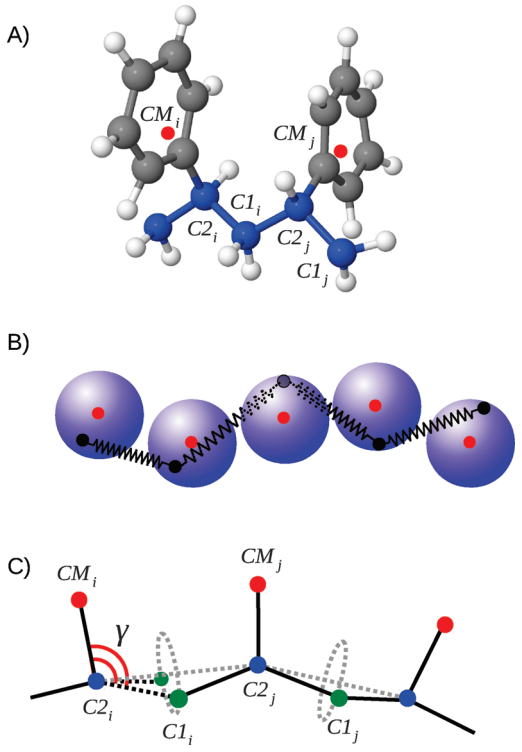

Figure 1. (A) Schematic representation of two adjacent PS monomers. CM denotes the center-of-mass of the monomer, C1 a methylene carbon in the backbone, and C2 an asymmetric backbone carbon. (B) Schematic view of a sphere−spring representation of the PS polymer. (C) Essential geometrical elements required for the insertion of the atomistic position of the methylene (C1) and chiral (C2) carbons of PS in the present backmapping scheme. γ denotes the angle between the center-of-mass CM and the backbone carbons C1 and C2.

proposed a BM procedure for the above-mentioned CG model. A simple backmapping strategy for the (1:1) CG model of Qian et al.,[3] which does not carry information about the backbone structure, has not been reported until now. A description of this type of backmapping is the heart of the present work.

In the (2:1) schemes reported by others,[6,8] where each repeat unit is coarsened to two CG beads, the coordinates of the PS backbone atoms (see Figure 1) can be conserved in the CG representation. Hence, the CG structure is quite close to the atomistic one, and reverse mappings of coarse-grained PS are simpler than in the (1:1) case. The advantage of the adopted (1:1) CG scheme compared to (2:1) ones, besides the smaller number of interactions, is that all CG beads have the same mass, which is important for facilitating long time steps in CG simulations.[3]

The silica−PS composite studied in the present work is defined by one SiO_2 nanoparticle with a diameter of 4 nm and 202 identical polystyrene chains of 20 monomers ($N_L = 20$).[2,12] Each CG bead of the nanoparticle is formed by a single SiO_2 unit, located at the Si position. The chosen diameter leads to 873 of these beads. The PS superatoms in the adopted (1:1) coarse-graining are defined by one molecular repeat unit. Thus, we arrive at 4040 CG beads for the polymer. To derive the CG potential of the studied composite, we have adopted the in-house MD code IBIsCO.[13] The iterative Boltzmann inversion (IBI)[2] has been chosen to optimize the CG potential on the basis of bonded and nonbonded radial distribution functions (RDFs) of the atomistic reference, which have been generated from atomistic trajectory files. Detailed information on the IBI can be found elsewhere.[2,14,15] Most of the present calculations have been performed at a temperature (T) of 590 K, while an ambient pressure (P) of 101.3 kPa has been assumed throughout. The choice T = 590 K has been a result of the atomistic precursor simulations. In this resolution equilibrations at lower T would be too time-consuming.[12] The program code IBIsCO,[13] which works with tabulated numerical potentials, has been adopted for the CG part of our study. The Berendsen thermostat[16] (coupling time (τ) of 0.2 ps) and barostat (τ = 5.0 ps, isothermal compressibility of 1.0×10^{-6} kPa^{-1}) have been used. The nonbonded interactions were truncated beyond 1.5 nm; the neighbor list cutoff amounts to 1.6 nm. The time step is set up to 4 fs.

The atomistic MD simulations of the backmapped system have been performed with the YASP code.[17] The necessary force-field parameters for the polymer and the inorganic nanoparticle have been taken from our recent MD study of silica−PS composites.[12] In the final step of the backmapping we have allowed relaxation of the sample under isothermal−isobaric (NPT) conditions at P = 101.3 kPa and T = 590 K. These simulations have been executed with coupling times of 0.2 and 2.0 ps for the Berendsen thermostat and barostat. The time step now chosen amounts to 1 fs. A cutoff of 1.0 nm has been used for the nonbonded interactions. The MD results have been analyzed after relaxing the system for 2.0 ns.

BACKMAPPING STRATEGY

Backmapping of the studied silica−PS composite has been performed in two different steps in order to profit from the fixed atomic positions of the solid SiO_2 fragment. Here the BM step is straightforward and thus not commented on in the present work. The backmapping of the polymer consists of separate steps: First, atomistic fragments are threaded onto the coarse-grained backbone by geometrical operations. Second, the resulting atomistic structure is relaxed by a protocol of several very short molecular dynamics runs. The procedure is described in this section.

In an atomistic picture, each PS monomer has two backbone carbons, i.e., the methylene and chiral carbons C1 and C2 (see Figure 1A). The symbol CM in this diagram denotes the center-of-mass of a PS monomer. In the CG representation only the centers-of-mass and the chiralities of the beads are known. With the help of these data, our first BM step is the determination of the coordinates of the chiral −CHPh− carbon atom (C2 in Figure 1) of each monomer by a simple but rigorous approach. Ph states for a phenyl group. Then we locate the $-CH_2-$ methylene carbons (C1 in Figure 1) in the backbone of each monomer in a way that the desired chirality of all chain monomers is conserved. Knowledge of the coordinates of these two backbone carbons and the center-of-mass of the repeat unit is sufficient for a unique insertion of an atomistic template monomer with the help of simple rigid rotations and translations. Subsequently, we perform short MD runs to remove any overlap in the sample by gradually increasing nonbonded interactions.

Reduction of the Problem to a Sphere−Spring Model, Insertion of the C2 Atoms. For placing the chiral carbon atoms (C2) of the polymer, the average distance $R_s = \langle[(\vec{X}_{CM} - \vec{X}_{C2})^2]^{1/2}\rangle$ between CM and C2 positions in a monomer of atactic PS together with the average distance $L = \langle[(\vec{X}_{C2_i} - \vec{X}_{C2_j})^2]^{1/2}\rangle$ between C2 atoms of neighboring units are needed, where $\vec{X}_P$ symbolizes the Cartesian coordinates of point P. The indices i (from 1 to $N_L - 1$) and $j = i + 1$ denote chain monomers.

dx.doi.org/10.1021/ma2005958 |Macromolecules 2011, 44, 5520–5526

Table 1. Average Values and Associated Standard Deviations for the Bond $C2_i-C1_i$ and Angles $C2_i-C1_i-C2_j$ and $CM_i-C2_i-C1_i$ in the Considered Nanocomposite Sample[a]

$C2_i-C1_i$ (nm)	0.156 ± 0.003
$C2_i-C1_i-C2_j$ (deg)	114.89 ± 3.31
$CM_i-C2_i-C1_i$ (deg)	111.63 ± 3.51

[a] The data have been derived in the initial atomistic MD run at T = 590 K and P = 101.3 kPa.

They have been determined from the atomistic reference calculations,[12] which are the basis of the CG model: $R_s = 0.212 \pm 0.005$ nm and $L = 0.263 \pm 0.008$ nm (T = 590 K and P = 101.3 kPa).

To find the position of the C2 carbon atoms in the framework of the sphere−spring model, consider a single chain of N_L monomers. Around the center-of-mass CM of each bead, we define a sphere of radius R_s and moment of inertia I. These spheres are fixed in their position but are allowed to rotate around their center. Then we choose one random point $\vec{X}'_{C2}$ on each sphere as an initial guess for the C2 position. The points $\vec{X}'_{C2}$ of two neighboring beads are connected by a harmonic spring potential $V(l) = k(L-l)^2/2$, where L is the average equilibrium distance between two neighboring C2 atoms, l is their actual distance, or length of the spring, and k = 1 N/m is the force constant (see Figure 1B). Since most springs will not be in their equilibrium position in the initial configuration, each C2 carbon atom experience a net force from its two neighbors. Sphere i will rotate under the influence of the torque $\vec{\tau}_i = \vec{R}_{s,i} \times \vec{F}_i$, where $\vec{R}_{s,i}$ is the vector connecting $\vec{X}'_{C2}$ of the ith sphere with $\vec{X}_{CM_i}$ and $\vec{F}_i$ is net force on it. The equation of motion governing the rotation of sphere i is $\vec{\tau} = I\vec{\alpha}_i$, where $\vec{\alpha}_i$ is angular acceleration.

Defining $\vec{\omega}_i$ as the angular velocity, $\Delta\theta_i = {}^1/_2\alpha_i\Delta t^2 + \omega_i\Delta t$ is the angular displacement of the ith sphere within the step Δt. To avoid uncontrolled rotations and hence divergence problem, we have chosen Δt, I, and k in a way that each sphere will rotate only a few degrees per time step. This criterion is fulfilled by setting I = 1 kg m^2, k = 1 N/m, and Δt = 0.1 s. At each time step the initial angular velocity is reset to zero, hence each sphere rotates around its rotational axis which is in the direction of $\vec{\tau}_i$. Thus, each sphere rotates so as to reduce the net force on it, which is equivalent to a steepest-descent energy minimization (SDEM) in orientation space. Thereby the potential energy of the system decreases until its minimum is reached. The SDEM procedure continues up to a point where the potential energy of the sphere−spring model cannot be reduced further. This threshold is reached when the largest residual torque falls below 0.001 N m. At this point the lengths of all the springs are within 0.015 nm of their equilibrium length L. According to our experience, the final chain configuration does not depend sizably on the initial random configuration. As a quantitative example, we applied the sphere−spring model for a CG chain with 100 monomers. These tests have been performed for 10 different initial configurations. The mean distance of predicted positions for each C2 atoms from the corresponding average position was 0.11 nm.

Up to now we have determined the position of the C2 carbon atoms in each fragment only with the knowledge of the centers of mass and the distances R_s and L. Thereby, we have localized half of the backbone atoms.

Insertion of the C1 Atoms. The next step in our backmapping procedure is the insertion of the methylene carbon $C1_i$ of each fragment i which is bonded to $C2_i$ and $C2_j$. This triplet of atoms defines the bond angle $C2_i-C1_i-C2_j$. Insertion of C1 requires

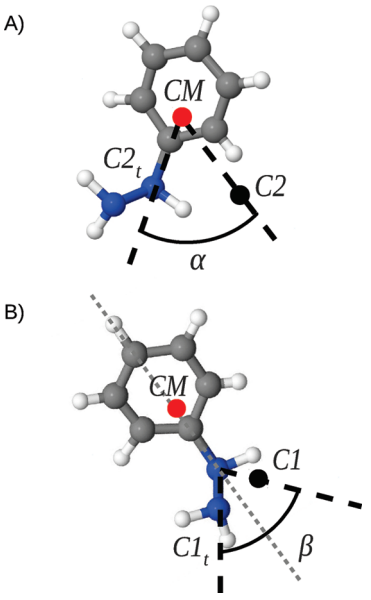

Figure 2. (A) Rotation of a molecular fragment under consideration of CM to shift the atomistic template carbon $C2_t$ to the backmapped position C2. (B) Rotation around the CM−C2 axis to shift the methylene carbon $C1_t$ to position C1.

knowledge of the chirality of the monomers. We use the average values of the bond length $C2_i-C1_i$ and bond angle $C2_i-C1_i-C2_j$ which are known from the atomistic reference trajectory (Table 1). With these geometrical parameters a circle can be generated which defines the possible location of $C1_i$ (see Figure 1C). With the help of the angle γ defined by the triplet $CM_i-C2_i-C1_i$ also available from the atomistic trajectory (Table 1), the $C1_i$ position on the ring becomes constrained to two possibilities. The chirality (R or S) of the PS monomer determines on which side of the plane spanned by $CM_i-C2_i-C2_j$ the $C1_i$ carbon atom has to be placed. At this stage, the backbone has been fully constructed.

Insertion of the Whole Fragment. For the next BM step we need two coordinate triplets $\vec{X}_{C1_t}$, $\vec{X}_{C2_t}$, $\vec{X}_{CM_t}$, and $\vec{X}_{C1}$, $\vec{X}_{C2}$, $\vec{X}_{CM}$. The index t symbolizes that these coordinates refer to an atomistic template fragment extracted for example from the original atomistic reference trajectory (as the styrene repeat unit is very stiff, the template can also be taken from other sources). The other coordinate triplet is derived in the reverse mapping steps described above. First we shift the center-of-mass of the atomistic template $\vec{X}_{CM_t}$ to the backmapped coordinate $\vec{X}_{CM}$ leading to $\vec{X}_{CM_t} = \vec{X}_{CM}$. Next we match the $\vec{X}_{C2_t}$, $\vec{X}_{C1_t}$ coordinates to the $\vec{X}_{C2}$, $\vec{X}_{C1}$ set estimated in the reverse mapping (Figure 2). The set $\vec{X}_{C2_t}$, $\vec{X}_{CM}$, $\vec{X}_{C2}$ defines a plane, $\vec{n}$ being the normal vector. By a rotation of the molecular fragment around $\vec{n}$ by an angle α (Figure 2A), we move $\vec{X}_{C2_t}$ to its correct position $\vec{X}_{C2}$. Finally, we rotate the whole fragment around the C2−CM axis by an angle β and move $\vec{X}_{C1_t}$ to $\vec{X}_{C1}$ (Figure 2B). At this point, we have a complete atomistic structure of the chain. Very recently, Ensing and Nielsen have adopted similar operations in their reverse mapping algorithm.[18] Note that the outlined procedure is applicable to all vinyl polymers whose repeat units can be considered as rigid. For flexible side chains, the procedure has to be modified. Some inter- and intrachain overlaps of the PS atoms are still possible at this stage. Also, some of the estimated bond lengths will not be in the desired range. The atomistic

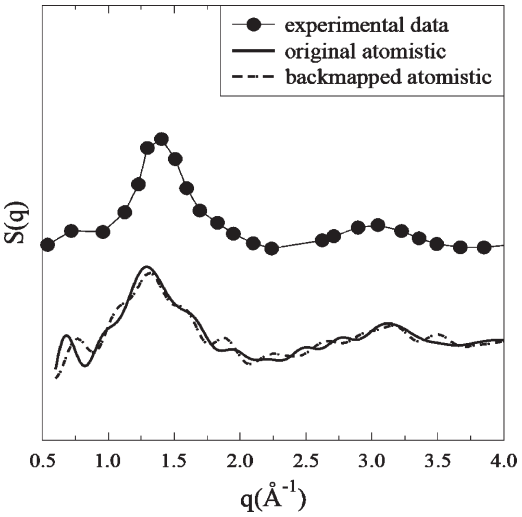

Figure 3. X-ray structure factor $S(q)$ of backmapped bulk atactic PS chains of 20-mers (continuous line) and of the original atomistic system (dashed line), both at $T = 300$ K and $P = 101.3$ kPa. Above the simulation results is shown experimental[21] X-ray scattering pattern (filled circles) of atactic PS (16 monomer per chain, $T = 323$ K).

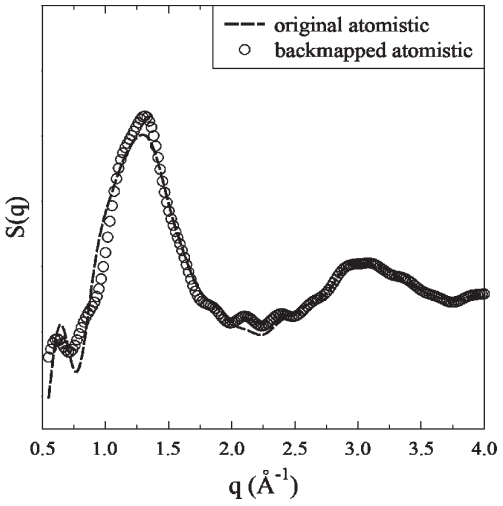

Figure 4. X-ray structure factor of the PS component of the silica−PS nanocomposite in backmapped (continuous line) and the original atomistic[12] (dashed line) resolutions. The simulations have been performed for 20-mer chains at $T = 590$ K and $P = 101.3$ kPa.

simulation protocol to further relax the system is described in the next subsections.

NVT Simulations at Zero Temperature. Initially, zero-temperature MD simulations at constant volume and using the Berendsen thermostat (coupling time (τ) of 0.5 fs and bath temperature 0 K, the average temperature is 18.78 K) are performed with a time step $\Delta t = 0.005$ fs. The number of time steps Δt is 500 000, leading to a time for this stage of 2.5 ps. To optimize the bonded part of the potential, all nonbonded interactions in the atomistic force field are switched off during this simulation. In the course of this zero-temperature run all bond lengths and angles reach their equilibrium values. The average displacement of the monomers (centers-of-mass) from their initial positions does not exceed 0.01 nm during the whole zero-temperature run so the overall chain conformation as produced by the CG simulation is preserved.

Soft-Core Simulations for the Nonbonded Interactions. In the next stage of relaxation, the nonbonded interactions are reintroduced. However, a soft-core potential is applied to them to remove possible overlaps, concatenation, and spearing between different PS chains. As this method has been commented on in detail in recent backmapping studies of the group,[19,20] only a short overview will be given here. The soft-core potential is implemented into the YASP package[17] by replacing the short-range part (<0.32 nm) of the nonbonded Lennard-Jones potential by a cubic spline. The spline coefficients have been determined to reproduce the original potential energy and its derivative at the crossover distance as well as to have a finite value V_0 and a zero derivative at a distance of zero. With this choice atoms can pass through each other, thereby allowing a relaxation of high-energy configurations. The value of V_0 is increased in four steps (50, 100, 500, and 1000 kJ/mol). For each value, an MD simulation of 50 000 time steps $\Delta t = 0.005$ fs (i.e., 0.25 ps) is performed at a bath temperature of 590 K, with a temperature coupling time of 0.5 fs. Finally, the full nonbonded potential without soft core is restored. In these runs, the time step is gradually brought from its initial value 0.005 fs to the regular value of 1 fs. For every new value of Δt (typically an order of magnitude larger than the last) we run an NVT simulation over 50 000 time steps.

These runs amount to ∼75 ps of simulation time. The last step of relaxation is a standard constant-volume simulation of 1 ns. For the subsequent data analysis, another 1 ns simulation is used.

■ VALIDATION OF THE BACKMAPPING PROCEDURE

To test the ability of the present BM method to generate structural features of polymer chains, the structure factor $S(q)$ obtained through the Fourier transform of the atomistic radial distribution functions (RDF) of the reverse mapped PS model (without a nanoparticle) was compared with the measured X-ray diffraction pattern in Figure 3. In contrast to the 590 K simulations performed for the nanocomposite, we now have chosen $T = 300$ K to allow a better comparison with experiment with has been performed at 328 K. The measured intensity pattern[21] is well reproduced by the simulated one. The so-called polymerization peak, which is mainly due to intermolecular correlations between backbone atoms, appears at the same wavenumber ($q = 0.75$ Å^{-1}) as in experiment. The main peak, known as amorphous peak, which arises primarily from phenyl−phenyl correlations and appears at 1.4 Å^{-1} in the experimental data, is centered at a bit lower wavenumber in the calculated $S(q)$, around 1.35 Å^{-1}. There is a third calculated peak at $q = 3.1$ Å^{-1} that is also found in experiment. In Figure 3, the calculated structure factor for the reference atomistic simulation is shown, too. Its good agreement with the reverse mapped X-ray pattern shows that the difference between calculated and experimental structure factors, namely the amplitude and relative position of the peaks, is due to the adopted force field. These results confirm the ability of the reverse mapping procedure to reproduce realistic structural features of polymers.

Then we applied the BM method to the PS component of the silica−PS composite, where the necessity of a fast and simple reverse mapping scheme comes from. The structure factor of the reverse mapped PS component of the nanocomposite calculated by a Fourier transform of RDFs of coarsened monomers is shown in Figure 4. The excellent agreement with calculated X-ray

dx.doi.org/10.1021/ma2005958 |*Macromolecules* 2011, 44, 5520–5526

Table 2. Total Mass Density (ρ) of the Silica−PS Composite, Radius of Gyration (R_g), and End-to-End Distance (R_0) of the Atactic PS Component of the Studied Nanocomposite As Derived in the Atomistic Reference Simulation, the CG Simulation, and the Atomistic Simulation after Backmapping[a]

	original atomistic	coarse-grained	backmapped atomistic
density (kg/m^3)	980.91 ± 0.08	978.24 ± 0.03	978.95 ± 0.03
radius of gyration, $\langle R_g^2\rangle^{1/2}$ (nm)	0.95 ± 0.01	1.01 ± 0.01	0.99 ± 0.01
end-to-end distance, R_0 (nm)	2.25 ± 0.05	2.43 ± 0.06	2.43 ± 0.05

[a] For each quantity we have given the MD inherent error bars, calculated as standard deviation of the quantity around corresponding average value over 1000 frames.

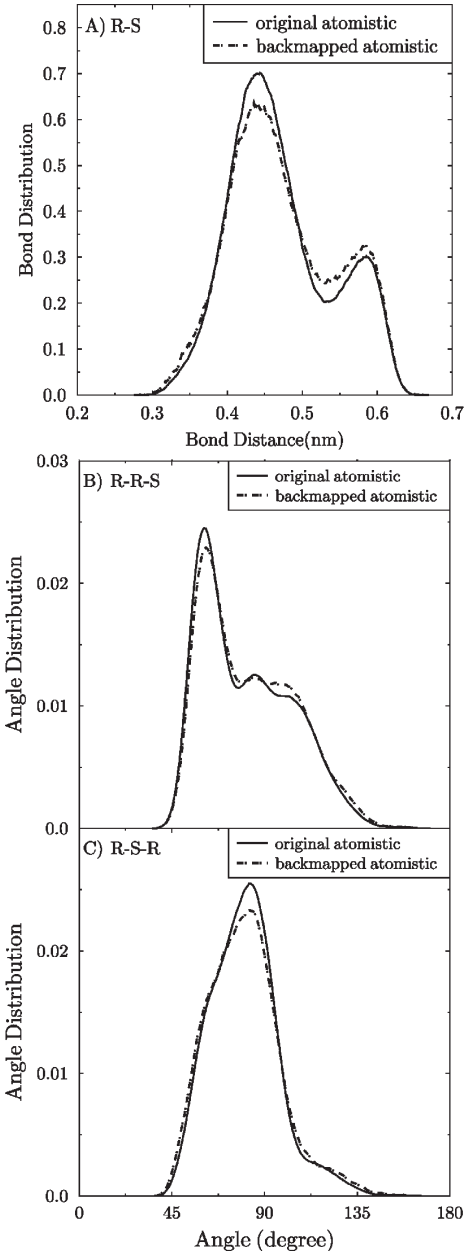

Figure 5. Distribution function of the R−S (A) bond and R−R−S (B) and R−S−R angles (C) of atactic PS according to the original atomistic target simulation[12] and the backmapping approach.

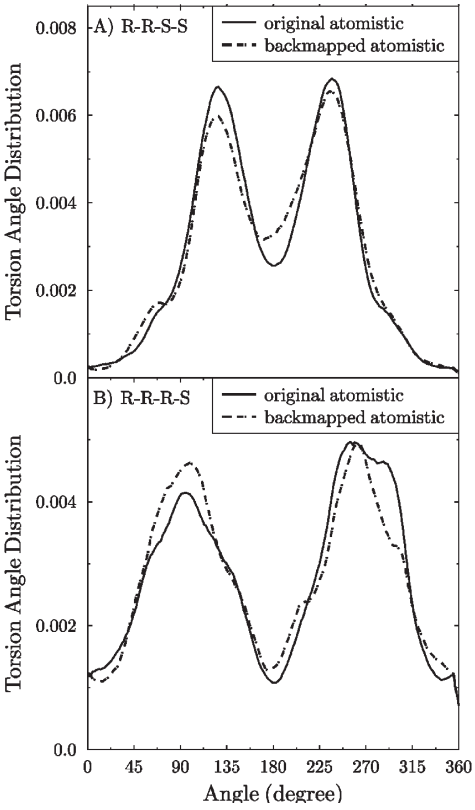

Figure 6. Distribution function of the intrachain torsional angles R−R−S−S (A) and R−R−R−S (B) of atactic PS according to the reference atomistic MD[12] and after backmapping.

pattern of the original atomistic simulation (after about 2 ns of equilibration) indicates that structural properties of the PS chains are successfully retrieved upon backmapping the CG structure also in the presence of the nanoparticle. There is a small prepeak at q = 0.7 Å^{-1}, close to the wavenumber where the polymerization peak appears in the experimental data of pure PS. The main peak at q = 1.25 Å^{-1} is followed by a third peak at approximately q = 3 Å^{-1}.

NPT simulation of the backmapped silica−PS composite at the same pressure and temperature as adopted in the CG simulations results in an overall density (ρ) of 979.0 kg/m^3, which is in good agreement with atomistic simulation data (ρ = 980.9).[12] In Table 2 we relate the two atomistic ρ (i.e., original atomistic simulation,[12] after backmapping) to the CG value. In addition to the density other structural parameters (i.e., radius of gyration $\langle R_g^2\rangle^{1/2}$ and end-to-end distance (R_0)) as derived by the three MD variants are compared. We see that the backmapped R_g and R_0 are close to the reference atomistic values as well as to the CG values.

In Figure 5, we have plotted the distribution functions of the R−S bond as well as the R−R−S and R−S−S angles of

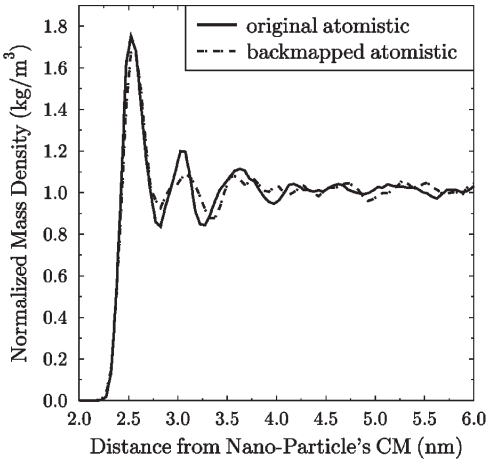

Figure 7. Radial profile of the normalized mass density $\rho(r)/\rho(\text{bulk})$ of the polymer component of the silica−PS composite from the refrence atomistic MD[12] simulation and after backmapping.

polystyrene in the nanocomposite calculated in the reference atomistic simulation (used to develop the CG model)[12] and after backmapping (T = 590 K). R and S refer to monomers of the two possible chiralities. The BM distribution functions are of the same widths as derived in the atomistic reference simulation. Even the height of the atomistic curves is reproduced with sufficient accuracy by the present reverse mapping. The same good agreement is also observed for the other bond and angle distribution functions not shown here. Figure 6 gives the distribution functions for the torsional angles R−R−S−S (top diagram) and R−R−R−S (bottom diagram) derived in the reference atomistic run and the backmapped simulations. The good agreement between the two profiles indicates that the reverse mapping retains the correct tacticity of the chains. As this must be the case by construction of the BM procedure, the agreement is evidence for a correct implementation and execution of it.

As last example, the normalized radial mass density ($(\rho(r)_n = \rho(r)/\rho(\text{bulk})$) of the polymer around the nanoparticle in the silica−PS nanocomposite is compared (Figure 7) for the original atomistic simulation[12] and after backmapping, where $\rho(\text{bulk})$ stands for the bulk density of a neat polymer sample. The positions of the $\rho(r)_n$ maxima and minima are reproduced with good accuracy. The strong first maximum followed by at least one second peak is characteristic for attractive nanoparticle−polymer interactions.[12] It reflects an increased ordering of the surface near polymer chains and thus the formation of an interlayer. This calculated interlayer region for the silica−PS composite is in agreement with other studies.[22−24] The observed difference in the amplitude of maxima and minima in the density profile of original atomistic and the backmapped simulations can be attributed to atomistic data not fully equilibrated. The fast CG simulations now allow further relaxation.

■ CONCLUSIONS

A new simple backmapping procedure has been proposed for vinyl polymers whose repeat units can be considered rigid. As a test, it has been applied for the polymer part of a silica−polystyrene nanocomposite. The present backmapping scheme makes use of elementary geometrical and classical mechanics considerations. It requires neither expensive evaluations of the potential energy nor force determinations at individual atoms. Global structural properties of the backmapped PS, such as the gyration radius and end-to-end distance, reproduce atomistic reference simulations. The structure factor of bulk PS after backmapping is in good agreement with experimental measurements as well as with that calculated in reference atomistic simulations. The same good agreement is also observed for the polymer part of the nanocomposite. Comparison with experiment is here not possible due to the lack of data.

Most of the published backmapping procedures have been designed for CG schemes in which the atomistic backbone information is preserved by the chosen bead locations.[5,10,19,25−27] In our BM procedure, this information is not needed in the coarse-graining scheme. The main advantage of our BM method compared to existing schemes is that it requires less structural information. The sphere−spring model allows the reinsertion of atomistic templates via rigid rotations.

The backmapped atomistic system prepared at this step does not have strong overlaps between the atoms. This is achieved by the energy minimization step in the sphere−spring model. Moreover, it correctly takes into account the tacticity of the chain. Santangelo et al.[10] proposed a BM scheme for PS where the concept of quaternions is used to correctly orient atomistic diads into the CG structure. They used position restraints and additional repulsive particles at the centers of phenyl rings together with scaled Lennard-Jones potentials to further relax the chains and to remove catenation of phenyl rings. The present scheme is somewhat simpler. It requires the insertion of rigid atomistic fragments (from a library) into the CG configuration. The fragments are taken from a short atomistic trajectory and have minimum-energy structure. Catenation of phenyl rings rarely happens in the proposed method because the backmapping scheme places the centers of mass of the monomers, which are close to the phenyl-ring centers, away from each other. Therefore, the probability of catenation is much reduced already in the stage of geometrical reconstruction. The main source of possible overlap in the backmapped configuration is due to the end groups, which have only one neighboring monomer. This widens the range of space where C1 and C2 carbons of the end groups can be found, increasing the chance to overlap with nearby atoms. The relative orientation of the phenyl rings, however, is not optimized in the insertion algorithm. Any possible overlap originating from this is efficiently relaxed in the ensuing molecular dynamics protocol.

Spyriouni et al.[5] proposed yet another backmapping method for atactic polystyrene. Compared to this scheme, our technique requires fewer parameters to be matched during the reverse mapping procedure. To sum up, with respect to the relaxation as well as the removal of intra- and interchain overlaps the present reverse mapping follows the lines of well established backmapping tools. In contrast to other schemes, we make explicit use of simplifications that are caused by rigid side groups. This allowed us to work with a minimum of structural information.

A comparison of the structural properties of the backmapped system with the reference simulations of the same atomistic model and also with experimental data, where available, indicates the ability of the outlined BM procedure to reproduce realistic chain configurations.

■ AUTHOR INFORMATION

Corresponding Author

*E-mail: a.ghanbari@theo.chemie.tu-darmstadt.de.

■ ACKNOWLEDGMENT

The authors are grateful to Tinashe Ndoro for providing the atomistic trajectory as well as to Mohammad Rahimi and Frédéric Leroy for their useful comments. Special thanks from A.G. to Jaber Dehghany for many informative discussions and his encouragement. Finally, we thank Sabine Philipp for critically reading the manuscript. This work has been funded by the EU project NanoModel (211778) as well as by the Deutsche Forschungsgemeinschaft through the Priority Programme 1369 Polymer-Solid Contacts: Interfaces and Interphases.

■ REFERENCES

(1) Müller-Plathe, F. *Soft Matter* **2003**, *1*, 1.
(2) Reith, D.; Pütz, M.; Müller-Plathe, F. *J. Comput. Chem.* **2003**, *24*, 1624.
(3) Qian, H.-J.; Carbone, P.; Chen, X.; Karimi-Varzaneh, H. A.; Liew, C. C.; Müller-Plathe, F. *Macromolecules* **2008**, *41*, 9919.
(4) Milano, G.; Müller-Plathe, F. *J. Phys. Chem. B* **2005**, *109*, 18609.
(5) Spyriouni, T.; Tzoumanekas, C.; Theodorou., D. N.; Müller-Plathe, F.; Milano, G. *Macromolecules* **2007**, *40*, 3876.
(6) Harmandaris, V. A.; Reith, D.; van der Vegt, N. F. A.; Kremer, K. *Macromol. Chem. Phys.* **2007**, *208*, 2109.
(7) Sun, Q.; Faller, R. *Macromolecules* **2006**, *39*, 812.
(8) Harmandaris, V. A.; Adhikari, N. P.; van der Vegt, N. F. A.; Kremer, K. *Macromolecules* **2006**, *39*, 6708.
(9) Sun, Q.; Faller, R. *Comput. Chem. Eng.* **2005**, *29*, 2380.
(10) Santangelo, G.; Di Matteo, A.; Müller-Plathe, F.; Milano, G. *J. Phys. Chem. B* **2007**, *111*, 2765.
(11) Tschöp, W.; Kremer, K.; Hahn, O.; Batoulis, J.; Burger, T. *Acta Polym.* **1998**, *49*, 75.
(12) Ndoro, T. V. M.; Voyiatzis, E.; Ghanbari, A.; Theodorou, D. N.; Böhm, M. C.; Müller-Plathe, F. *Macromolecules* **2011**, *44*, 2316.
(13) Karimi-Varzaneh, H. A.; Qian, H. J.; Chen, X.; Carbone, P.; Müller-Plathe, F. *J. Comput. Chem.* **2010**10.1002/jcc.21717.
(14) Carbone, P.; Karimi-Varzaneh, H. A.; Chen, X.; Müller-Plathe, F. *J. Chem. Phys.* **2008**, *128*, 064904.
(15) Reith, D.; Meyer, H.; Müller-Plathe, F. *Macromolecules* **2001**, *34*, 2335.
(16) Berendsen, H. J. C.; Postma, J. P. M.; Van Gunsteren, W. F.; Dinola, A.; Haak, J. R. *J. Chem. Phys.* **1984**, *81*, 3684.
(17) Müller-Plathe, F. *Comput. Phys. Commun.* **1993**, *78*, 77.
(18) Ensing, B.; Nielsen, S. O. In *Trends in Computational Nanomechanics Transcending Length and Time Scales*; Dumitrica, T., Ed.; Springer: Berlin, 2010; Vol. 9, p 25.
(19) Karimi-Varzaneh, H. A.; Carbone, P.; Müller-Plathe, F. *J. Chem. Phys.* **2008**, *129*, 154904.
(20) Carbone, P.; Karimi-Varzaneh, H. A.; Müller-Plathe, F. *Faraday Discuss.* **2010**, *144*, 25.
(21) Londono, J. D.; Habenschuss, A.; Curro, J. G.; Rajasekaran, J. J. *J. Polym. Sci., Part B: Polym. Phys.* **1996**, *34*, 3055–3061.
(22) Vogiatzis, G.; Voyiatzis, E.; Theodorou, D. N. *Eur. Polym. J.* **2010**10.1016/j.eurpolymj.2010.09.017.
(23) Barbier, D.; Brown, D.; Grillet, A. C.; Neyertz, S. *Macromolecules* **2004**, *37*, 4695.
(24) Brown, D.; Mele, P.; Marceau, S.; Alberola, N. D. *Macromolecules* **2003**, *36*, 1395.
(25) Queyroy, S.; Neyertz, S.; Brown, D.; Müller-Plathe, F. *Macromolecules* **2004**, *37*, 7338.
(26) Mulder, T.; Harmandaris, V. A.; Lyulin, A. V.; van der Vegt, N. F. A.; Michels, M. A. J. *Macromol. Theory Simul.* **2008**, *17*, 393.
(27) Hess, B.; Leon, S.; van der Vegt, N. F. A.; Kremer, K. *Soft Matter* **2006**, *2*, 409.